TECHBRIEF

Finite Element Analysis of UHPC: Structural Performance of an AASHTO Type II Girder and a 2nd-Generation Pi-Girder

FHWA Publication No. of this TechBrief: FHWA-HRT-10-079

NTIS Accession No. of the report covered in this TechBrief: PB2011-100864

FHWA Contact: Ben Graybeal, HRDI-40, 202-493-3122, benjamin.graybeal@dot.gov

This document is a technical summary of the unpublished Federal Highway Administration (FHWA) report, *Finite Element Analysis of Ultra-High Performance Concrete: Modeling Structural Performance of an AASHTO Type II Girder and a 2nd Generation Pi-Girder*, available only through the National Technical Information Service, www.ntis.gov.

Objective

This TechBrief highlights the results of a research program that developed finite element analysis modeling techniques applicable to ultra-high performance concrete (UHPC) structural components.

Introduction

UHPC is an advanced cementitious composite material that tends to exhibit superior properties such as exceptional durability, increased strength, and long-term stability.[(1–3)]

This research program is aimed at developing general finite element concepts within a commercially available finite element package to facilitate the development of UHPC structural systems. This investigation focused on calibrating the proposed finite element models to a series of completed full-scale structural tests on existing UHPC structural components, including a prestressed UHPC American Association of State Highway Transportation Officials (AASHTO) Type II girder and a prestressed UHPC second-generation pi-girder.

U.S. Department of Transportation
Federal Highway Administration

Research, Development, and Technology
Turner-Fairbank Highway Research Center
6300 Georgetown Pike
McLean, VA 22101-2296

www.tfhrc.gov

Finite Element Models and UHPC

Table 1 presents example mechanical properties for the type of UHPC investigated in this study. The properties far surpass those normally associated with concrete. The concrete damaged plasticity (CDP) model was primarily employed to model the constitutive behaviors of UHPC.[4,5] It assumes isotropic damage elasticity combined with isotropic tensile and compressive plasticity to represent the inelastic behavior of concrete. Formation of tensile microcracks is represented macroscopically with a softening stress-strain relationship, and the compressive plastic response is represented by stress hardening followed by strain softening beyond the ultimate compressive strength.

Table 1. UHPC Material Properties.

Property	Value
Unit weight	160 lb/ft^3 (2,565 kg/m^3)
Modulus of elasticity	7,650–8,000 ksi (53–55 GPa)
Poisson's ratio	0.18
Compressive strength	29 ksi (200 MPa)
Post-cracking tensile strength	1.4–2.3 ksi (9.7 to 15.9 MPa)
Ultimate tensile strength	0.007–0.010

Figure 1 depicts the typical assumed uniaxial stress-strain relationship of UHPC. The CDP parameters were calibrated through comparison to experimental structural test results, including three on an I-girder and a series on the second-generation pi-girder. The three-dimensional (3-D) finite element models of the I-girder and pi-girder test specimens are illustrated in figure 2 and figure 3.

Figure 1. UHPC Uniaxial Material Model.

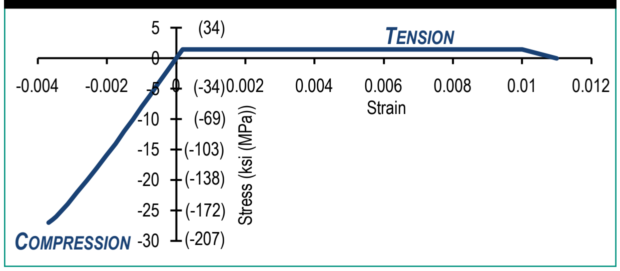

Figure 2. 3-D Finite Element Models of I-Girders 80F, 24S, and 14S.

Figure 3. 3-D Finite Element Models of Pi-Girder and Pi-Girder with Joint.

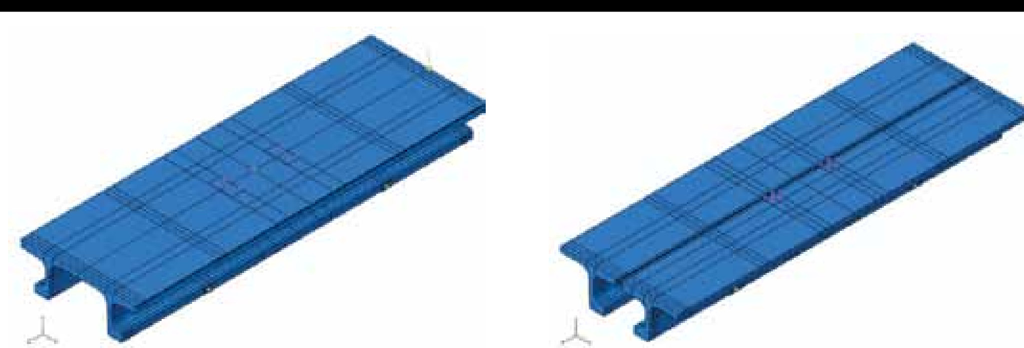

In the pi-girder models, nonlinear springs replaced actual diaphragms and linear springs replaced elastomeric pads in order to facilitate modeling. Some idealized scenarios were also investigated to complement the experimental results and to suggest potential future optimizations. Parametric studies were presented to address issues such as mesh sensitivity, concrete smeared cracking model, different tension stiffening definitions, grouting material, and contact interaction. Finite element model-predicted results were compared with experimentally captured measurements.

Figure 4 and figure 5 present a comparison of midspan deflection and strain responses of the I-girder 80F.

Figure 6 and figure 7 present the predicted deflections of the I-girders 24S and 14S along six instrumentation lines spaced in the longitudinal direction in comparison with the experimental measurements that were modified by excluding possible linear elastic deformation

Figure 4. I-Girder 80F: Deflection at Midspan.

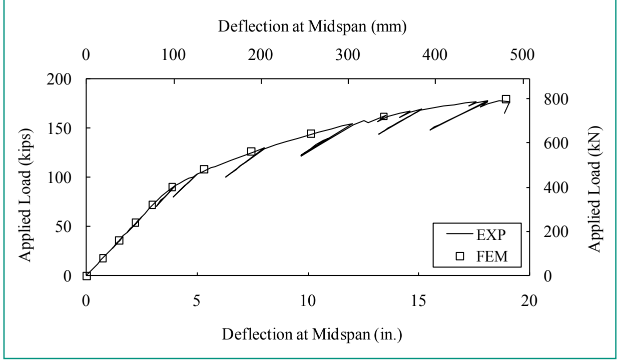

Figure 5. I-Girder 80F: Longitudinal Strains at Midspan.

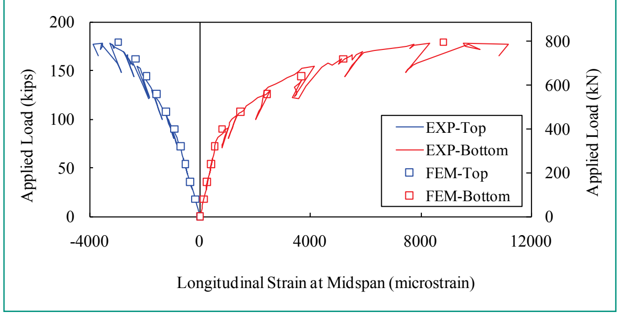

Figure 6. I-Girder 24S: Deflection Along Specified Instrumentation Lines.

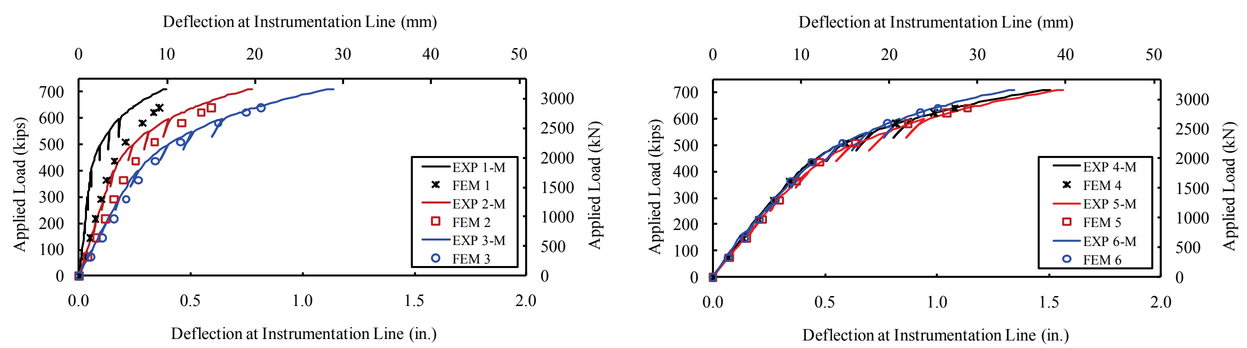

Figure 7. I-Girder 14S: Deflection Along Specified Instrumentation Lines.

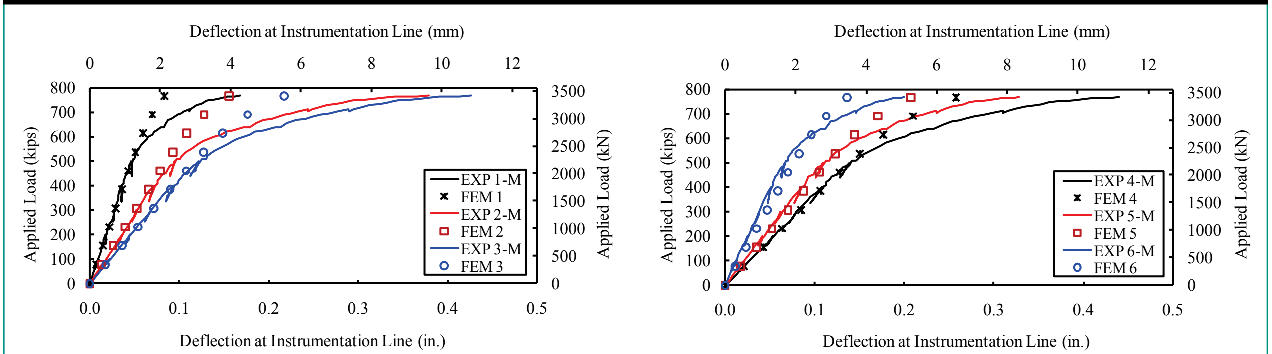

of the test supporting systems. In figure 7, the slippage of the prestressing strands accounts for the larger nonlinear deflection observed in the experiment.

Figure 8 through figure 13 present the experimental and finite element results on deflection, longitudinal strain, leg spreading at midspan, and diaphragm force for the pi-girder. Figure 14 through figure 19 show the experimental and finite element results for the pi-girder with joint.

Figure 20 presents the finite element-predicted maximum principal stress contours of the pi-girder and pi-girder with joint at midspan cross section in deformed shapes under applied loads of 340 kips (1,512 kN) and 428 kips (1,904 kN), respectively.

The results show that CDP models using appropriate parameters in any of the three types of tension stiffening definitions can capture both linear and nonlinear behaviors of the I-girders and pi-girders reasonably well. The assumed elastic-perfectly-plastic tensile stress-strain relationship for UHPC used in the CDP models is reasonable.

Figure 8. Pi-Girder: Deflection of Bulb at Midspan.

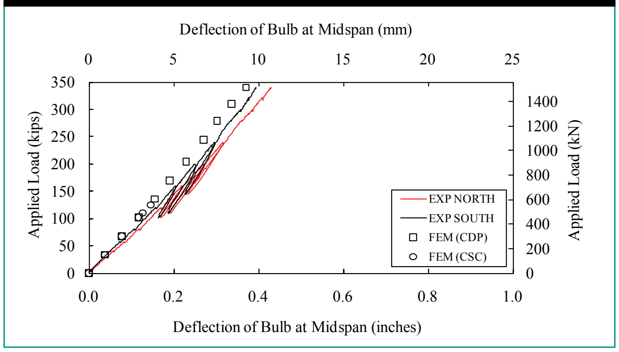

Figure 9. Pi-Girder: Deflection of Middeck at Midspan.

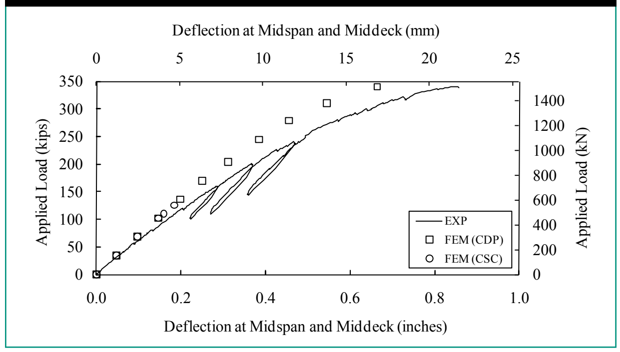

Figure 10. Pi-Girder: Longitudinal Strain on Bulb Bottom Surface at Midspan.

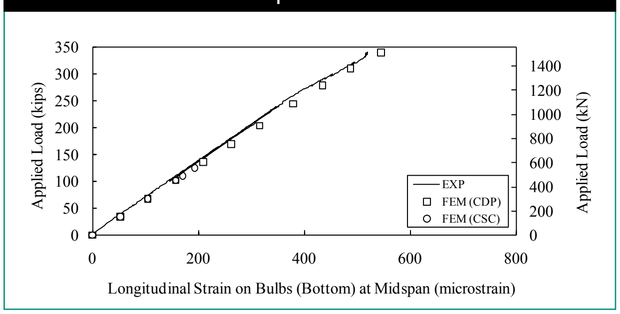

Figure 11. Pi-Girder: Longitudinal Strain on Deck Surface Immediately Above Web at Midspan.

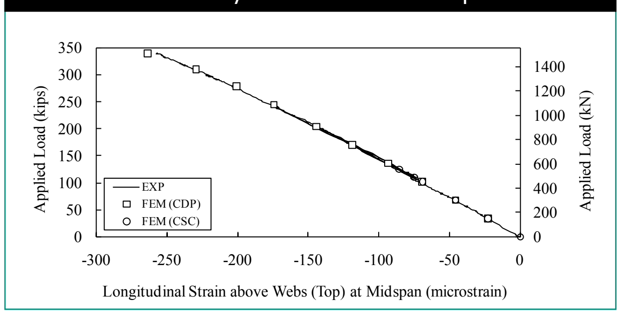

Figure 12. Pi-Girder: Bulb Lateral Spreading at Midspan.

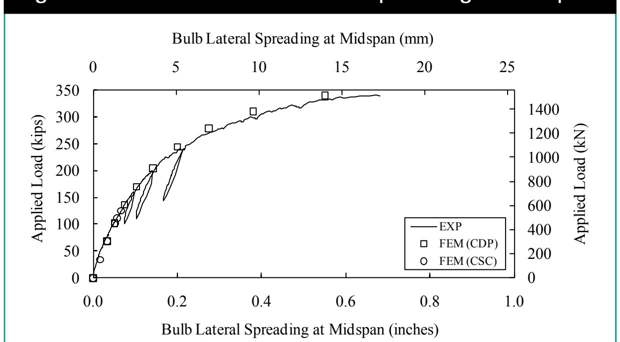

Figure 13. Pi-Girder: Diaphragm Force.

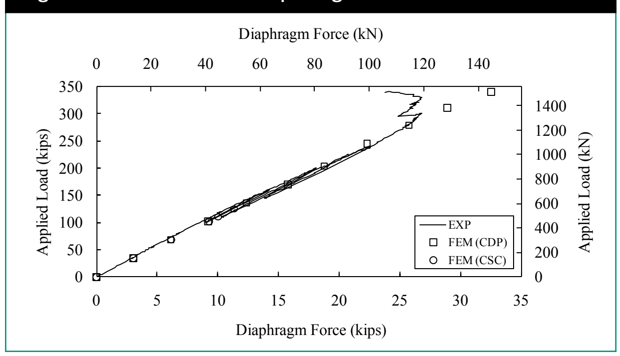

Figure 14. Pi-Girder with Joint: Deflection of Bulbs at Midspan.

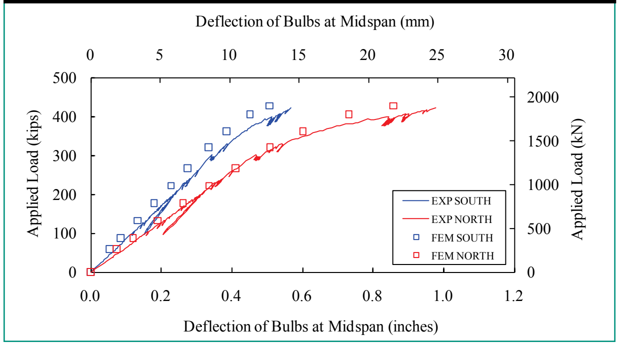

Figure 15. Pi-Girder with Joint: Deflection of Deck Near Joint at Midspan.

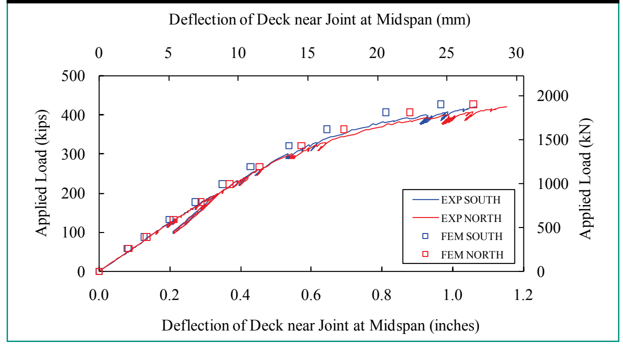

Figure 16. Pi-Girder with Joint: Longitudinal Strain on Bulb Bottom Surface at Midspan.

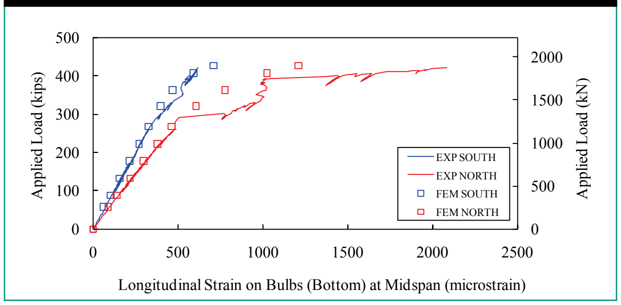

Figure 17. Pi-Girder with Joint: Longitudinal Strain on Deck Top Surface Immediately Above Webs at Midspan.

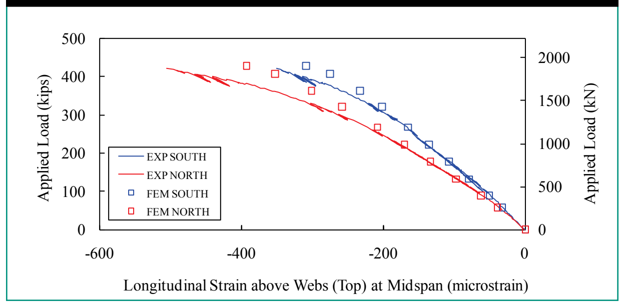

Figure 18. Pi-Girder with Joint: Bulb Lateral Spreading at Midspan.

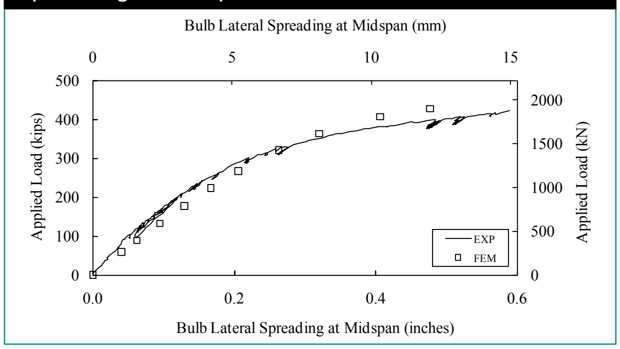

Figure 19. Pi-Girder with Joint: Diaphragm Force.

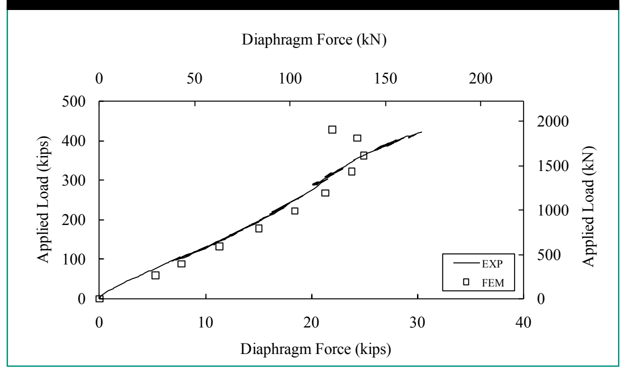

Figure 20. Stress Contours from Modeled Pi-Girder Test Simulations.

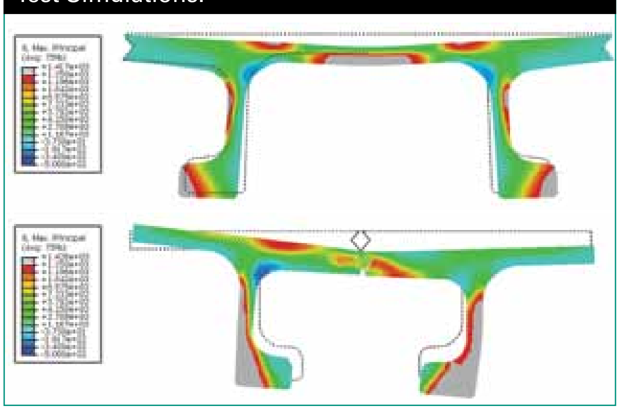

Conclusions

The CDP model replicates the observed responses better than the concrete smeared cracking model in the prestressed UHPC I-girders and second-generation pi-girders. The CDP model, using appropriate parameters in any of three types of tension stiffening definitions, can capture both linear and nonlinear behaviors of the modeled tests. The proposed modeling techniques, including nonlinear spring diaphragms, linear spring pads, automatic stabilization, and contact interaction, were demonstrated to be effective. The failure mechanics in the physical tests have been investigated with additional information provided by the models.

Future Research

The research completed in this study has led to the initiation of a number of related studies. A family of UHPC pi-girder cross sections applicable to a range of span lengths and configurations is under development. Combined effects of discrete and fiber reinforcements on UHPC are under investigation. Other full-scale UHPC structural component tests are being modeled in order to gain a greater understanding of the performance of precast UHPC components and field-cast UHPC connections.

References

1. Graybeal, B. (2006). *Material Property Characterization of Ultra-High Performance Concrete*, Report No. FHWA-HRT-06-103, Federal Highway Administration, McLean, VA.
2. Graybeal, B. (2006). *Structural Behavior of Ultra-High Performance Concrete Prestressed I Girders*, Report No. FHWA-HRT-06-115, Federal Highway Administration, McLean, VA.
3. Graybeal, B. (2009). *Structural Behavior of a 2nd Generation Ultra-High Performance Concrete Pi-Girder*, Federal Highway Administration, McLean, VA.
4. Chen, W.F. (1982). *Plasticity in Reinforced Concrete*, McGraw-Hill, New York.
5. SIMULIA™. (2009). Abaqus Software and Documentation, Version 6.9-1, Dassault Systèmes, Providence, RI.

Researchers—This study was completed by contract staff at the Turner-Fairbank Highway Research Center under the direction of Ben Graybeal. Additional information can be gained by contacting him at 202-493-3122 or in the FHWA Office of Infrastructure Research and Development located at 6300 Georgetown Pike, McLean, VA 22101.

Distribution—The unpublished report covered in this TechBrief is being distributed through the National Technical Information Service, www.ntis.gov.

Availability—The report will be available in November 2010 and may be obtained from the National Technical Information Service, www.ntis.gov.

Key Words—Ultra-high performance concrete, UHPC, Finite element analysis, FEA, Abaqus, Concrete smeared cracking, and Concrete damaged plasticity.

NOVEMBER 2010

FHWA-HRT-10-079
HRDI-40/11-10(150)E